Materials Science Forum Vols. 740-742 (2013) pp 357-360

doi:10.4028/www.scientific.net/MSF.740-742.357

Raman investigation of aluminum-doped 4H-SiC

S. Juillaguet[1, a], P. Kwasnicki[2,b], H. Peyre[1,c], L. Konczewicz[1,d], S. Contreras[2,e], M. Zielinski[3,f] and J. Camassel[2,g]

[1] Université Montpellier 2, Laboratoire Charles Coulomb UMR 5221, F-34095, Montpellier cedex 5, France

[2] CNRS, Laboratoire Charles Coulomb UMR 5221, F-34095, Montpellier cedex 5, France

[3] NOVASiC, Bourget du Lac and CRHEA-CNRS, 06560 Valbonne, France

[a] sandrine.juillaguet@univ-montp2.fr, [b] Pawel.kwasnicki@univ-montp2.fr, [c] herve.peyre@univ-montp2.fr, [d] Leszek.konczewicz@univ-montp2.fr, [e] sylvie.contreras@univ-montp2.fr, [f] mzielinski@novasic.com, [g] jean.camassel@univ-montp2.fr

Keywords: Raman spectroscopy, SIMS measurements, 4H-SiC, Fano interference effects, p doping.

Abstract. Raman scattering spectra have been collected on p-type 4H-SiC samples doped with aluminum up to 5×10^{19} atoms per cubic cm. The distortion and asymmetry of FTA modes which appear in the low frequency range has been probed in great details. We show that, using standard Fano formulae with three parameters per mode, one can successively fit all FTA modes profiles in the concentration range $2\times10^{16} - 5\times10^{19}$ Al.cm^{-3}.

Introduction

Raman spectroscopy is a well-known technique to perform analyses of the residual doping in silicon carbide (SiC) samples [1, 2]. Most of the time, for n-type material one focuses on the line shape and frequency shift of the LOPC (Longitudinal Optical Phonon Plasmon Coupled) mode. For p-type doping and especially in the case of heavily doped material, the change in LOPC line is not suitable. One rather focuses on the Fano interference effect between the FTA (Folded Transverse Acoustic) phonon modes and the continuum of electronic transitions [3].

In this work, we analyse the effect of Fano interferences between the continuum of electronic transitions and the FTA modes in low-doped p-type 4H-SiC samples. We work in the range 2×10^{16} to 5×10^{19} Al.cm^{-3} and show that the change in Fano parameters can be used as a measure of the p-type doping for aluminum (Al) concentrations as low as 2×10^{18} cm^{-3}.

Experimental details

Samples. We consider a series of eight Al-doped 4H-SiC layers grown on 8° off-axis, n-type, 4H-SiC substrates. They have been labelled A to H. The growth was done using chemical vapour deposition (CVD) in a hot wall, horizontal and resistively heated, reactor [4]. Hydrogen was used as carrier gas and silane and propane as Si and C precursors, respectively. The growth temperature and pressure were 1550°C and 200 mbar, respectively. Aluminum was used for p-type doping using tri-methyl-aluminium (TMA) diluted in hydrogen as precursor. The thickness of the epitaxial layers ranged from 3.5 to ~ 5 μm and, as a reference or witness sample (W) a piece of non-intentionally doped 4H-SiC epitaxial layer grown on 4H-SiC was used.

SIMS. Secondary Ion Mass Spectroscopy measurements were done using a Cameca IMS 5f spectrometer and a O_2^+ primary ion source. The impact energy was 15 keV. The secondary beam high voltage was 4.5 kV and the mass resolution was fixed at M/ΔM = 2000. The investigated atomic masses (and specific detection limits) were: $^{13}C^+$ (matrix), $^{28}Si^{++}$ (matrix), $^{11}B^+$ (few 10^{15} to 10^{14} cm^{-3}), $^{14}N^+$ (10^{18} to few 10^{17} cm^{-3}) and $^{27}Al^+$ (few 10^{14} to few 10^{13} cm^{-3}). The size of craters was 150 x 150 μm^2 and their depth was measured using a Dektak 150 profile-meter. The RSF (Relative Sensitivity Factors) used to calibrate the concentration profiles were: 1.1×10^{19}, 4.1×10^{20} and

2.97×10^{17} for $^{11}B^-$, $^{14}N^+$ and $^{27}Al^+$, respectively. They were defined from reference samples in which the concentration profiles were known, using the $^{28}Si^{++}$ isotope signal as matrix reference. Whatever the sample, the counting levels for $^{11}B^+$ was low, with corresponding boron concentrations lower or equal to 10^{16} cm^{-3}. Concerning the $^{14}N^+$ isotope, we found a concentration of few 10^{18} cm^{-3} in the substrate but systematically below (or equal to) the detection limit in the epitaxial layers (i.e. lower or equal to few 10^{17} cm^{-3}). Finally, the concentration of incorporated Al in the epitaxial layer ranged from 10^{16} to 2×10^{19} cm^{-3} (see Table 1), while the Al level in the substrate was only few 10^{15} cm^{-3}.

Raman. Micro-Raman measurements were done at room temperature, in the backscattering configuration, using an Aramis micro-Raman spectrometer from Jobin Yvon-Horiba and the 632.8 nm line of a He-Ne laser as excitation source.

Table 1: Aluminum concentrations measured by SIMS on the different samples. Also given are the epilayer thickness, the average C(V) values and the hole concentration determined by Hall measurements at room temperature.

Samples	W	A	B	C	D	E	F	G	H
Al concentration (cm^{-3})	Al-free	2×10^{16}	10^{17}	2×10^{18}	4×10^{18}	10^{19}	$1\text{-}2\times10^{19}$	$2\text{-}3\times10^{19}$	5×10^{19}
Thickness (μm)	4.8	3.5	3.5	4.6	4.4	3.6	5	3.5	3.5
$[N_A\text{-}N_D]$ Average C(V) measurement (cm^{-3})		2×10^{16}	2×10^{16}	2×10^{18}	2×10^{18}	2×10^{18}	10^{19}	10^{19}	10^{19}
Hole concentration (cm^{-3})				8.2×10^{17} 1.1×10^{18}		8.7×10^{17} 1.1×10^{18}		1.8×10^{18} 1.9×10^{18}	8.5×10^{18} 9.1×10^{18}

Results and discussions

In Fig.1 we show a comparison of the experimental Raman spectra obtained on samples A to H in the range 100-300 cm^{-1}. At low frequency, we first notice that a broad continuous band appears which increases in intensity vs Al doping. This is a pure electronic effect in which a virtual electron-hole pair is created by an incoming photon. During excitation, the hole scatters to some empty state in the topmost valence band and the electron-hole pair recombines with a different energy. This energy difference appears as an electronic Raman shift. Of course, when the free hole concentration increases, the scattering probability increases and so does the Raman intensity. This is clearly seen in Fig.1.

Accompanying this pure electronic effect, a shift and change in the Raman shape of the FTA (2/4) modes appear when the Al concentration increases. This is best seen in Fig.2 which is a zoom of Fig.1 in the experimental range 190-210 cm^{-1}. In both cases, the fractional numbers between brackets refer to the wave vector in the extended zone scheme. In the witness (W) and low-doped sample (A) the two modes appear at 196.7 cm^{-1} and 204.5 cm^{-1}, respectively, in good agreement with previous determination [2]. Increasing the Al concentration, the situation complicates and clear interference effects manifest between the continuum of electronic transitions and the FTA modes.

These interferences arise because of the coupling in the Raman transitions matrix between the virtual electron-hole pair and the phonon states. Let us call the lower and higher frequency doublet components as FTA^- and FTA^+, respectively, the Fano interferences profile of these FTA doublet modes will then be theoretically described by the simple Fano formula [2, 5]:

$$I(\omega) = I^+(\omega) + I^-(\omega) = \frac{(q_+ + \varepsilon_+)^2}{(1+\varepsilon_+^2)} + \frac{(q_- + \varepsilon_-)^2}{(1+\varepsilon_-^2)}.$$

In this expression $q_{+/-}$ are the so-called asymmetry parameters. $\varepsilon_{+/-}$ are the dimensionless frequency defined by $\varepsilon_{+/-} = \frac{(\omega - \Omega_{0+/-} - \delta\Omega_{+/-})}{\Gamma_{+/-}}$. $\Omega_{0+/-}$ are the Raman shift of the phonon frequency without interference. $\delta\Omega_{+/-}$ and $\Gamma_{+/-}$ are the peak shift and the broadening due to the interference effect, respectively. These characteristics parameters are related to the Raman matrix element and the hole concentration [3, 5].

Using these Fano formulae with three parameters per mode, we could successively fit all FTA modes profiles in the concentration range 2×10^{16} – 5×10^{19} Al.cm^{-3}. This is shown in Fig.3 for two different samples: A (low-doped) and H (high-doped, respectively). The experimental results are shown by crosses and the fit by the solid line. The different fit parameters are given in the insert. Finally, the change in asymmetry parameters vs Al concentration is shown in Fig. 4 for all samples.

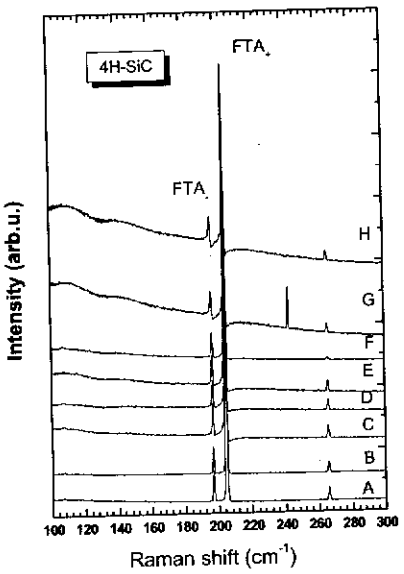

Figure 1: Comparison of Raman scattering spectra collected at room temperature in the range 100-300 cm^{-1}. From sample A to H, the SIMS Al concentration changes from 2×10^{16} to 5×10^{19} (Table 1).

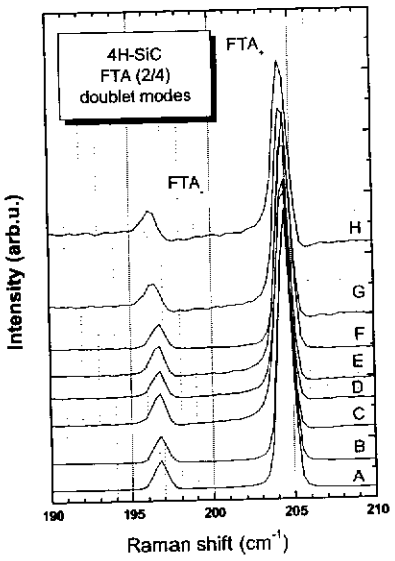

Figure 2: Effect of Fano interference on the shape of the FTA modes at 196.7 cm^{-1} and 204.5 cm^{-1}.

Notice the clear correspondence between this parameter value and the incorporated Al concentration.

Since they should be also related to the hole concentration, electrical measurements were done using standard DC methods on four samples. The resistivity was measured in the Van der Pauw configuration and, for Hall Effect measurements, a magnetic field of 1 Tesla was used. The results, which have been reported in Table 1, show the qualitative agreement with the results of C(V) measurement and/or the Al concentrations determined by SIMS. For unknown samples, this shows that the hole concentration can be directly evaluated from the analysis of interference effects in micro-Raman spectra.

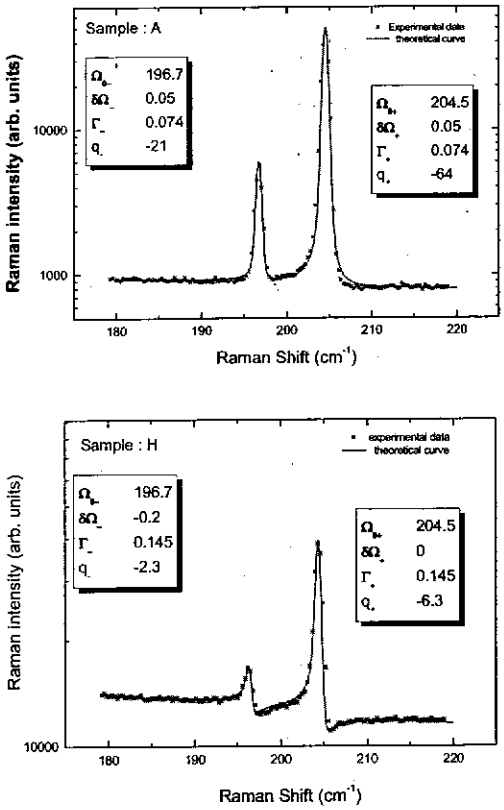

Figure 3: Example of fits obtained on two differently doped sample A (low-doped) and H (high-doped).

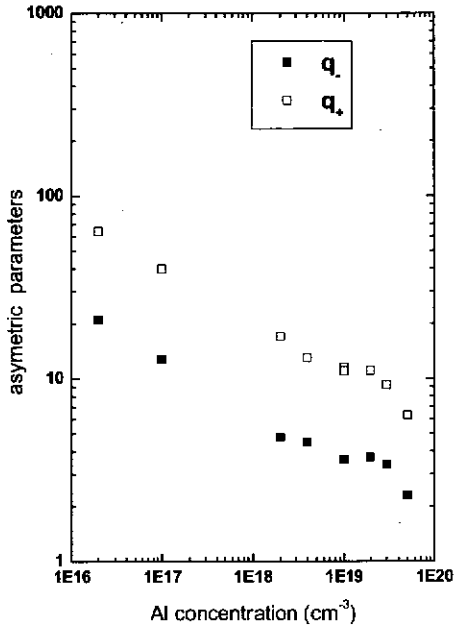

Figure 4: Trend in asymmetry parameters vs Al concentration.

Conclusion

Raman scattering spectra were measured on p-type 4H SiC samples doped with aluminum (Al). Increasing the Al concentration, the distortion and asymmetry of FTA modes appear in the low frequency range. Using standard Fano formulas with three parameters per mode, one can successively fit all FTA modes profiles in the concentration range $2\times10^{16} - 5\times10^{19}$ Al.cm^{-3}. Our results shown that the analysis of asymmetric parameters can be an interesting tool to determine the hole concentration in 4H-SiC samples down to ~ $1x10^{18}$ holes per cubic centimeter.

Acknowledgment We greatly thank the EU for partial support in the framework of the NETFISiC project (Grant No. PITN-GA-2010-264613).

References

[1] M.V. Klein, *Ligth scattering in solids*, chapter 4, M. Cardona ed., Springer, Berlin (1975).

[2] S. Nakashima and H. Harima phys. stat. sol. (a) **162**, (1997) 39.

[3] H. Harima T. Hosoda and S.I. Nakashima, Mater. Science Forum **338-342**, (2000) 607.

[4] A. Leycuras, Mater. Science Forum **338-348**, (2000) 241.

[5] U. Fano, Phys. Rev. **124**, (1961) 1866.